Chem. Senses 28: 499–508, 2003

High-resolution Analysis of the Spatio-temporal Activity Patterns in Rat Olfactory Bulb Evoked by Enantiomer Odors

M.J. Lehmkuhle, R.A. Normann and E.M. Maynard

Center for Neural Interfaces, Bioengineering Department, University of Utah, 20S 2030E BPRB Rm #506, Salt Lake City, UT 84112, USA

Correspondence should be sent to: Richard A. Normann, Center for Neural Interfaces, Bioengineering Department, University of Utah, 20S. 2030E. BPRB Rm. #506, Salt Lake City, UT 84112. e-mail: normann@utah.edu

Abstract

Understanding how mammals process olfactory stimuli has motivated the development of tools and techniques which permit the simultaneous study of finely structured spatial and temporal patterns of neural activity. A technique is described that uses an array of 32 penetrating microelectrodes implanted bilaterally into the dorsal aspect of rat olfactory bulb to investigate the responses of mitral and tufted neurons to stimulation with simple enantiomer odor pairs at a number of concentrations. It is shown that stable, simultaneous recordings from up to 49 single- and multi-units can be performed for periods of up to 14 h. We show that such odors evoke unique spatial and fast-temporal activity patterns which may subserve odor discrimination. This technique is extensible to other systems neuroscience investigations of olfactory sensory processing.

Key words: electrophysiology, encoding, ensemble, mitral cells, multielectrode, population

Introduction

An understanding of the mechanisms by which the mammalian olfactory system can derive behaviorally relevant information from minute concentrations of odors involves studying the spatial and temporal patterns of neural activation in the mitral and tufted cell layer of the olfactory bulb (OB). A number of tools have been used to study the first stages of these spatio-temporal activity patterns in the mammalian olfactory bulb. Optical imaging (both intrinsic and dye enhanced) and functional magnetic resonance imaging have been used to record spatial and temporal changes in pre- and post-synaptic activity in the glomerular layer of the OB, and the synaptic connections between the olfactory receptor neurons and mitral and tufted (M/T) cells. The technique has revealed an odor- and concentration-dependent activation of specific glomeruli that is conserved across both hemispheres (Stewart *et al.*, 1979; Johnson *et al.*, 1998; Xu *et al.*, 2000; Belluscio and Katz, 2001; Rubin and Katz, 2001; Spors and Grinvald, 2002). However, limitations inherent in these techniques generally prevent direct imaging of either the M/T neurons, or of action potentials generated by these cells. Further, investigating the responses of both glomerular and cellular responses of the OB to near-threshold concentrations of odorants has not been studied.

Single and multiple microelectrodes have been used to record action potentials from M/T cells in mammals and the functional equivalent in insects (Moulton, 1963; Moulton and Tucker, 1964; Leveteau and MacLeod, 1966; Freeman, 1974b; Boulet *et al.*, 1978; Katoh *et al.*, 1993; Motokizawa, 1996; Bhalla and Bower, 1997; Kay and Laurent, 1999; Christensen *et al.*, 2000; Lei *et al.*, 2002). Although these techniques offer excellent temporal resolution, they report little information about how populations of these cells interact to contribute to concentration independent perception of odorants. Arrays containing large numbers of microelectrodes potentially could overcome the limitations of imaging and single microelectrode electrophysiological techniques by allowing the simultaneous recording of action potentials from many M/T neurons that are distributed spatially across the OB. An additional complication to the analysis of OB activity patterns is the well-documented phasic discharge that is correlated with the inhalation cycle of breathing (Onoda and Mori, 1980; Chaput, 1986; Kay and Laurent, 1999). This dynamic aspect of the activity pattern suggests that there is likely significant information about the delivered odor in the temporal structure of the response (Chaput and Holley, 1985).

In this study, we describe techniques that enable the investigation of the spatio-temporal firing patterns in the OB of a rat that is evoked by a number of enantiomer odors. The technique uses 32 penetrating microelectrodes, implanted into the dorsal aspect of OB of rat and simultaneous recording from a population of M/T neurons to stimulation with simple enantiomer odorants at low

concentrations. In order to permit the analysis of this data, we simultaneously monitored the animals' respiration. We demonstrate that stable, simultaneous recordings from up to 49 single- and multi-units can be performed for up to 14 h. This time frame is sufficiently long to investigate the response of ensembles of OB M/T cells to repeated delivery of enantiomer odors at a number of concentrations. We show that such odors evoke unique activity patterns which the rat could use to discriminate these odors. We conclude that microelectrode arrays, simultaneously recording action potentials from a large number of M/T neurons in the rat, offer a unique means of studying the ways ensembles of neurons represent and process olfactory information.

Materials and methods

Utah electrode array

The microelectrode arrays that were used in this study were constructed from single silicon wafers to form square matrices of up to 100 independent silicon electrodes spaced 400 μm apart (Cyberkinetics, Inc., Salt Lake City, UT) (Campbell *et al.*, 1991; Jones *et al.*, 1992). Each electrode is ~80 μm in diameter at the base and tapers to a point were only the insulation at the tip has been removed. Electrode tips are platinum coated and electrode shanks are insulated with silicon nitride or Parylene-C. One array of 16 electrodes, each 500 μm in length can be inserted into the dorsal aspect of each hemisphere of OB of rat (Figure 1). Two arrays can easily be implanted in a single rat allowing for the simultaneous recording from up to 32 micro-electrodes. Arrays are inserted using a rapid pneumatic insertion technique that has been shown to be effective at implanting high-density recording structures (Rousche and Normann, 1992).

Acute array implantation

Seven male Wistar rats (491–799 g) were anesthetized with an intraperitoneal injection of urethane (1250 mg/kg), placed on a heated surface, and fitted into a stereotaxic frame (David Kopf, 1430). Surgical access to the OB was made with a 7 mm diameter trephine. Two Utah electrode arrays (UEAs), measuring 2.0 mm on a side and containing 16 microelectrodes, were aligned over the two hemispheres of OB (Figure 2). Each array was pneumatically inserted with an impact inserter that was positioned over the arrays to achieve an insertion along an axis normal to the surface of the brain to a depth of 300 μm (Rousche and Normann, 1992). This corresponds to the average depth of the mitral cell layer from the surface of the OB (Paxinos, 1998). After insertion, any blood in the implant site was washed away with saline and the implant site perfused with saline to prevent dehydration. The arrays were then connected to a 100-channel amplifier and data acquisition system (Neural Signal Acquisition System, Cyberkinetics, Inc.). Each array

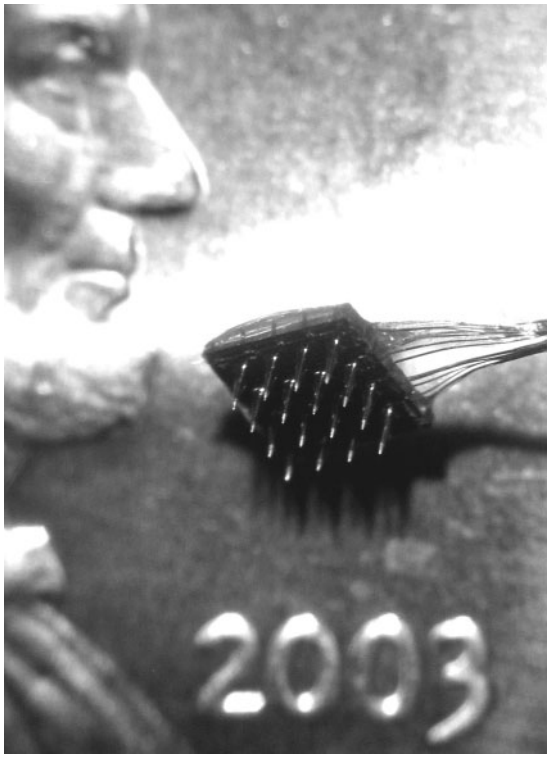

Figure 1 The Utah electrode array (UEA), a silicon multielectrode array.

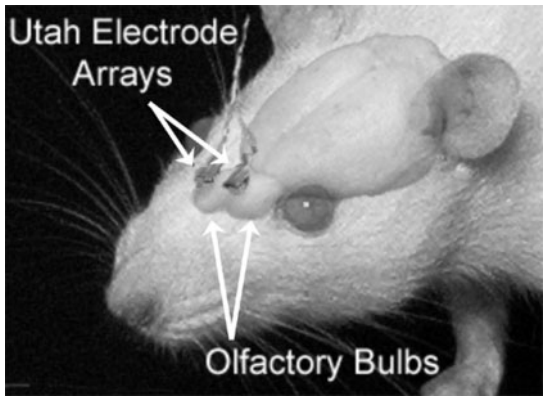

Figure 2 Two UEAs can be pneumatically implanted in the dorsal aspect of each hemisphere of OB of rat for simultaneous recordings from up to 32 microelectrodes. Electrodes are separated by 400 μm and are 500 μm in length.

was advanced using a micromanipulator attached to the back of the array such that the depth of the implantation was successfully fine-tuned to achieve the greatest number of electrodes simultaneously recording single- and multi-unit activity.

Odor stimulation

Pure odors were chosen as opposed to complex mixtures such that cellular responses were representative of the

simplest responses. Enantiomers—pairs of mirror-symmetric non-superimposable molecules that differ only in their optical activity (Linster *et al.*, 2001; Rubin and Katz, 2001)—were chosen based on their use in previous olfactory studies where they have been shown to elicit a response from glomeruli of the dorsal aspect of OB. Some of the odors used for stimulation include: (*R*)-(+)-limonene, (+L) (Sigma-Aldrich, Milwaukee, WI, 97+% pure); (*S*)-(–)-limonene, (–L) (Aldrich, 95+% pure); (*S*)-(+)-carvone, (+C) (Aldrich, 96% pure); (*R*)-(–)-carvone (–C) (Aldrich, 98% pure); (*S*)-(+)-2-butanol (+2B) (Acros Organics, Pittsburgh, PA, 99% pure); (R)-(–)-2-butanol (–2B) (Aldrich, 99% pure); at concentrations of 1, 5×10^{-2} and 5×10^{-5}% saturated vapor (v/v), all in their purest form available. Liquid dilution was used to achieve desired concentrations in mineral oil (Slotnick and Nigrosh, 1974). Odors were delivered in 30 s intervals for 1–2 s to free-breathing animals through a nose cone (Kopf, Tujunga, California) at 5 ml/min (animals A–E) or 20 ml/min (animals F and G) by a digitally controlled olfactometer built in-house (animals A–E) or available commercially (animals F and G; KNOSYS, Washington, DC) (Slotnick and Nigrosh, 1974; Slotnick and Ptak, 1977).

Electrophysiology

Signals from each electrode were amplified ×5000 gain, digitized at 30 KHz, filtered between 0.250 and 7.5 KHz, and simultaneously recorded on a Pentium-based computer (Neural Signal Acquisition System, Cyberkinetics, Inc.). The animal's phase of breathing and olfactometer solenoid position information were simultaneously recorded throughout the course of the experiment (6–14.3 h). Recordings were started in late-afternoon and continued through the night. The animal's phase of breathing was monitored through a sensitive thermistor circuit situated near the animal's mouth.

Data analysis

Spikes were clustered using a combination of an automated locally developed routine, which fits the observed waveforms using probabilistic models of spike waveform variability and manual principal component cluster analysis sorting methods (Offline Sorter, v. 2.3.1, Plexon, Dallas, TX). M/T cells were identified by; their distance from the surface of OB, and the magnitude of their action potentials (typically >50 μV peak to peak). Single- and multi-unit activity was analyzed with Neuroexplorer (Nex Technologies, v. 2.671, Littleton, MA) and Matlab, (Mathworks, release 13, Natick, MA).

Results

Our results represent simultaneous recordings from up to 32 microelectrodes of M/T cells from seven animals. In order to determine the efficacy of the UEA as a tool to reliably record spatio-temporal responses to a number of odorants we first examined the fundamental electrophysiological recording characteristics of the array. Table 1 summarizes the statistics of these electrophysiological recordings. Each recording session lasted an average of 9.7 h and was terminated when adequate data were acquired. We found this length of time adequate for recording the responses of neurons to ~200 trials of each of six odors per experiment. Over half (59%) of all implanted electrodes recorded single- and multi-units. On average, 33.4 units were recorded in a given experiment. Of the 121 electrodes recording single- and multi-unit activity in this analysis, 47 (39%) recorded one unit, 44 (36%) recorded two units, 23 (19%) recorded three units, 6 (5%) recorded four units, and 1 (1%) recorded five units. Figure 3 shows the average waveshape of three separate units recorded from a single electrode from animal G (top) and their respective interspike interval histograms (bottom). The mean firing rate of all units calculated over the entire course of each recording session was 14.1

Table 1 Summary of electrophysiological statistics

Animal ID	Length of each experiment (h)	No. of electrodes with activity	No. of single- and multi-units recorded	Mean firing rate[a]	Mean peak-to-peak voltage amplitude (μV)
A	6.0	10/25	14	22.0	98
B	7.9	14/25	25	15.3	118
C	6.2	10/32	20	16.2	154
D	12.4	18/32	41	16.3	153
E	10.0	20/32	37	20.9	159
F[b]	11.3	25/32	48	3.7	123
G[b]	14.4	24/32	49	4.2	95
Mean	9.7	58%	33	14.1	129

[a]Mean firing rate is calculated for each neuron over the entire length of the experiment (impulses/s).

[b]These experiments were executed with a different olfactometer from that used in animals A–E (see Materials and methods).

impulses per second and the mean peak-to-peak response amplitude was 129 μV. The mean of the distribution of signal-to-noise ratio was 3.5:1 (low 0.8:1; high 10.3:1; SD = 1.2) as calculated by dividing the peak-to-peak amplitude of the signal by the peak-to-peak amplitude of the noise. Once satisfied that we were able to repeatedly record from a number of large-amplitude units we then focused on the problem of respiratory modulation of responses.

It has been shown that OB neurons respond with a phasic discharge that is highly correlated to the phase of the animal's breathing (Figure 4a) (Chaput, 1986). We thus found it necessary to record the breathing cycle continuously throughout the recording sessions. Of the 234 single- and multi-units in this analysis, 181 (77%) showed a high correlation to the animals' breathing as can be seen in the raster and peristimulus time histogram (PSTH) of multi-unit activity recorded on a single electrode where the raster has been aligned to breathing in the absence of odorant stimulation (Figure 4a). Eighty cells (34%) responded to odorant stimulation with a change in firing rate irrespective of the phase of breathing. However, when the firing rate response of cells was aligned to the first inhalation in the presence of odorant stimulation, a larger number of cells (154; 66%) responded with a significant difference in firing rate (both positive and negative, Figures 4b and 5a–c). This result led us to align all trials in which odorant was present to the intake phase of breathing in the subsequent analyses. Units exhibited differential modulation to varying concentrations of the same odorant as can be seen in the PSTHs of a single-unit response to (–L) in concentrations of 1, 5×10^{-2} and 5×10^{-5}% (Figure 5a–c) as compared to the response to clean air (Figure 5d).

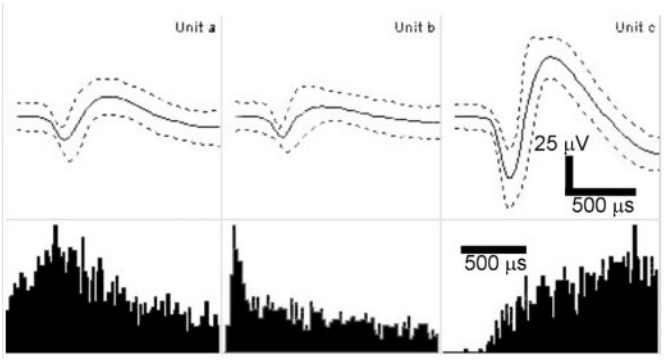

Figure 3 The average waveshape (solid lines) ± 3 SD (dashed lines) of three separable units on a single electrode within the UEA from animal G (top) and corresponding interspike interval histograms (bottom). Interspike interval count distributions (ordinate, bottom plots) are relative to each unit.

Generally, we were able to get stable recordings over long periods of time (6.0–13.6 h), however, in all experiments the level of spontaneous activity of all neurons was marked by increasing and decreasing firing rates over the course of the experiments. Figure 6 illustrates the 'waxing and waning' that was observed over time in every experiment. This figure represents the trial-by-trial firing rate of a single neuron in response to 306 presentations of (–L) over a 10 h recording session. Lighter shaded regions indicate an increase in the neural firing rate. Notice that although the firing rate seems to increase and decrease for blocks of trials (rows), three distinct 'bands' (columns) of activity are present throughout, representing the three breaths that occurred in the 2 s window.

Not only did neuron firing wax and wane but the amount

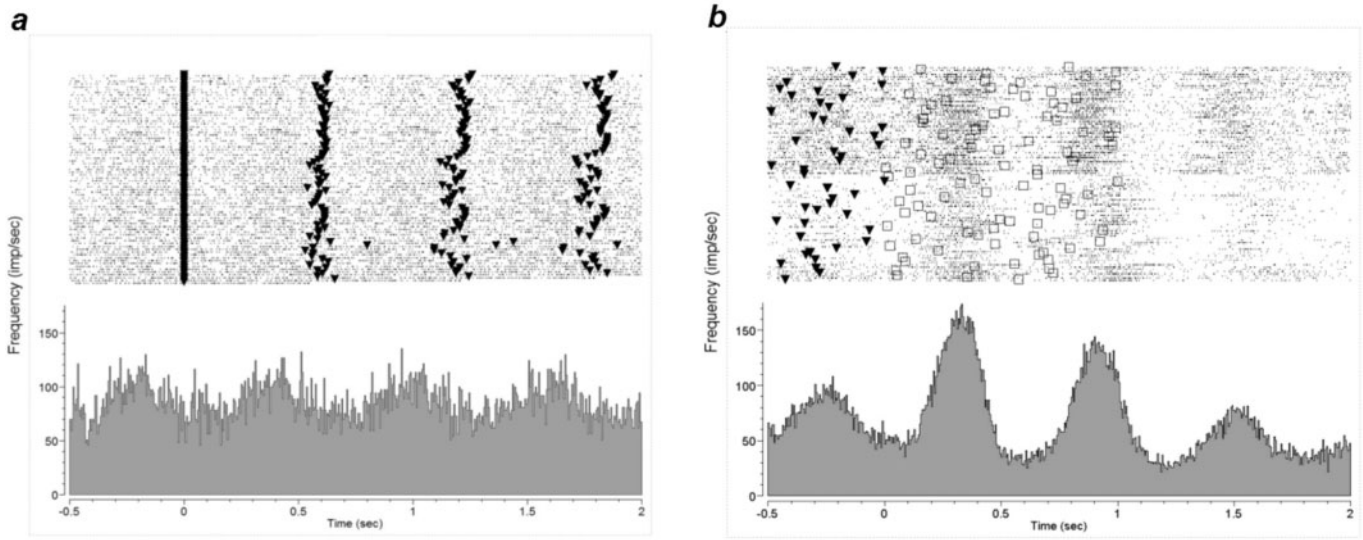

Figure 4 Rasters and peristimulus time histograms from multi-unit data of Animal E. **(a)** response to clean air **(b)** response to (S)-(–)-limonene, 1% v/v). Each row of the raster plot represents a trial. The PSTH is in 5 ms bins starting 0.5 s before the alignment and ending 2 s after the alignment. Triangles in (a) mark the alignment to each inhalation. Triangles and squares in (b) mark the start and end of odor presentation, respectively. Raster aligned to the first inhalation following the start of odor.

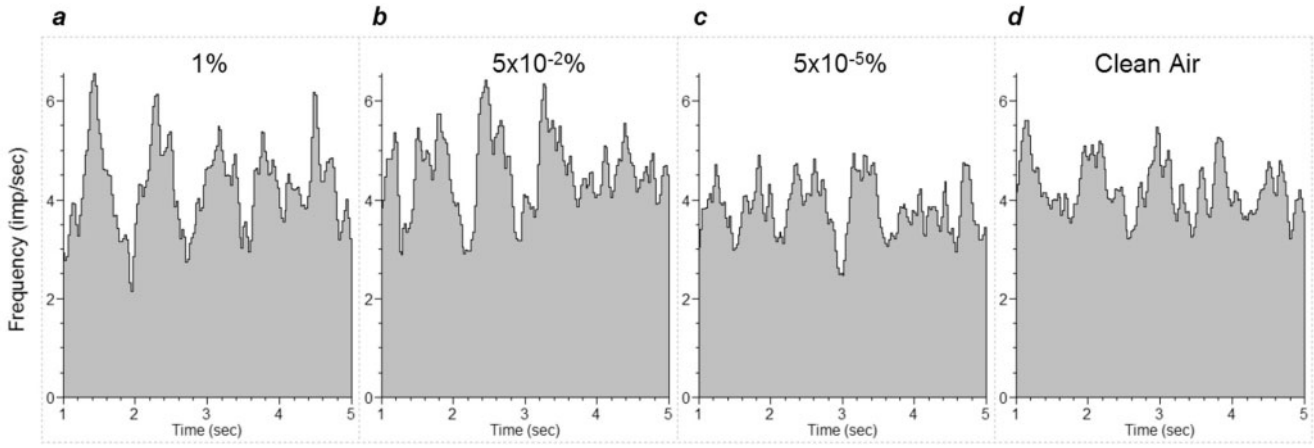

Figure 5 Peristimulus time histograms of the response of one single unit to a number of concentrations of (S)-(–)-limonene from animal G. **(a)** response to 1% v/v. **(b)** response to 5×10^{-2}% v/v. **(c)** response to 5×10^{-5}% v/v. **(d)** response to clean air. PSTHs are in 25 ms bins smoothed with three-bin gaussian window and have been aligned to the first inhalation following the start of odor (time = 0 s, not on graphs).

of time that each neuron was active varied. This led us to look at how long we could record each neuron over the course of an experiment. Figure 7 indicates the stability of these recordings and the viability of the experimental preparation by plotting the number of neurons that were active for a given time in 1-hour segments for each of seven animals. Notice that the majority of neurons were present over the entire length of each experiment.

We now were able to study how odorant stimulation affected M/T cell responses for a number of odors. It was found that cell responses were broadly tuned to odors. Of the 117 single- and multi-units (n = 4 rats; animals A, B, D and E) responding dynamically (an increase and/or decrease in firing rate) to three different enantiomer odorant pairs (six odors) at 1% (v/v) concentration; 18 (15%) did not respond to any of the odorants, 13 (11%) responded to one odorant, 5 (4%) responded to two odorants, 15 (13%) responded to three odorants, 12 (10%) responded to four odorants, 7 (6%) responded to five odorants and 47 (40%) responded to all six odorants. Of those cells responding to more than one odorant, the temporal characteristics of their response to each odor varied in the amount of activation and/or deactivation produced by the odorant presentation. This broad tuning to odors has been previously reported (Linster *et al.*, 2001; Rubin and Katz, 2001; Giraudet *et al.*, 2002). An example of a multi-unit response to 1% (–)-limonene used in this analysis can be seen in Figure 4b, recorded from animal E. In this same analysis the selectivity to odorants from all animals was as follows; 60 (51%) units responded to (+L), 89 (76%) units responded to (–L), 78 (67%) units responded to (+C), 73 (62%) units responded to (–C), 67 (57%) units responded to (+2B) and 70 (60%) units responded to (–2B). Since the number of neurons responding to different odors is nearly equal we investigated the spatio-temporal response dynamics of these neurons for a given odor.

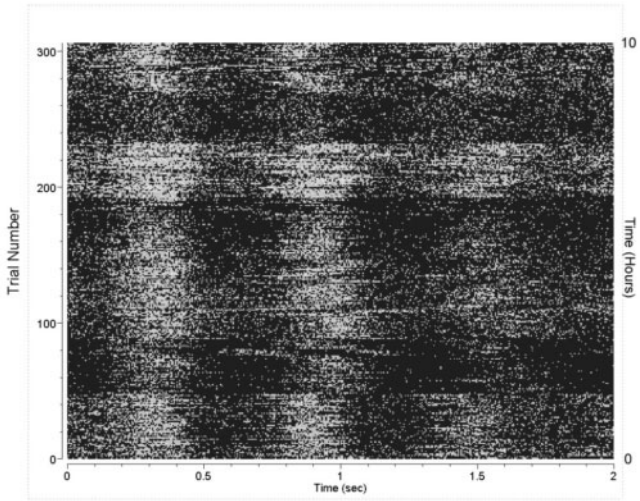

Figure 6 Trial-by-trial firing rate of a single neuron following 1% v/v (–L) odor presentation for 306 trials (over a course of 10 h). Each row represents a trial. Each column represents the firing rate in 5 ms bins. Responses are aligned to the first inhalation following odor presentation. Lighter shaded regions represent high firing rate, darker regions represent low firing rate. Firing rate for this cell: mean, 61.7 imp/s; high, 173.9 imp/s.

The multi-site simultaneous recording capabilities of the UEA allows us to investigate the spatio-temporal activity of a number of neuron's responses to odorants. This technique allows us to quantify spatial activation of a number of M/T neurons with high temporal resolution. Upon stimulating the animal with a number of trials of odorants we were able to create PSTHs for each neuron as a function of time and spatial position of each electrode in the OB. First we recorded the temporal aspects of each neuron. Figure 8a is the normalized false-color PSTH of the firing rate of 40 units recorded simultaneously from animal D aligned to inhalation cycles in the presence of clean air. Each row is a neuron and represents the PSTH of that neuron in 5 ms bins

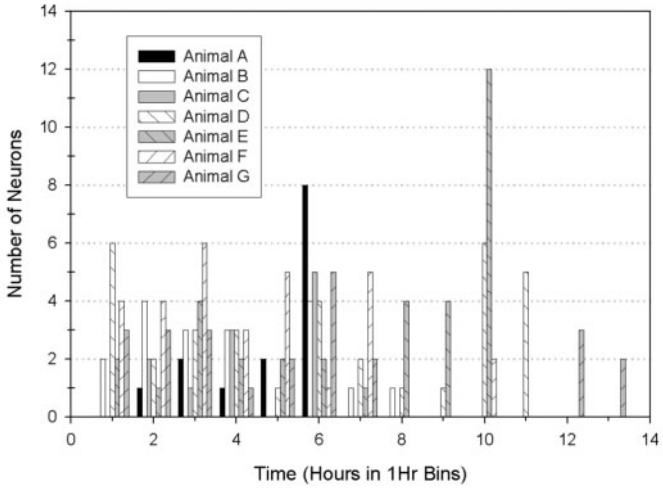

Figure 7 Neuron stability. Neuron activity from seven animals as a function of time for single- and multi-unit data in 1 h bins. Each bin represents the maximum time each neuron was active. The duration of each experiment is as follows: animal A, 6 h; B, 8 h; C, 6 h; D, 12.4 h; E, 10 h; F, 12.5 h; G, 14.3 h.

starting 0.5 s before and ending 1.5 s after the alignment. The color of the PSTH represents the normalized maximum firing rate for each neuron. Red colors indicate high firing rate, blue colors low firing rate. Figure 8b is the same analysis aligned to the first inhalation in the presence of 216 presentations of 1% v/v (–L). Not only can we see temporal firing characteristics linked to the inhalation phase of breathing in the responses to both odorant and air but the responses do not line up temporally; some neurons 'lead' and other neurons 'lag' with respect to each others response dynamics.

Next, we subtracted the PSTHs of the ensemble responses to clean air from the PSTHs of the ensemble responses to (–L), resulting in the raw difference PSTHs seen in Figure 8c. This process essentially removes the cyclic breathing component from the firing rate dynamics and results in differences evoked by differential activation. To determine if these differences are significant we compared the distribution of firing rates for each neuron in response to (–L) and clean air using the Wilcoxon nonparametric test at $P < 0.01$ for the specific time period from 0.250 to 0.750 s following the alignment. Those units' responses determined *not* to be significantly different between the two cases are marked by a star in Figure 8c.

Given the differential activation patterns as a function of time, we reorganized this information into each neuron's respective position within the electrode array as it was recorded *in vivo*. In order to display the spatial activation of these neurons we chose a single 5 ms bin from the difference plot 0.440 s following the alignment. This corresponds with a period of maximal difference in activation across all cells from the two cases from Figure 8a,b as determined by two-sample Kolmogorov–Smirnov goodness-of-fit hypothesis test for $P < 0.10$. We then took this 'window in time' and represented it with respect to its planar position within the UEA. Figure 9a shows a 4×4 grid aligned over each hemisphere of OB of rat with circles over many intersections. Each circle represents an electrode recording action potentials from OB. Each section of a single circle represents an isolated unit recorded on that electrode. The color of the sections of each circle show the amount of differential activation of that unit to (–L) versus clean air as seen in the plot of Figure 8c from time 0.440 to 0.445 s following the alignment. White color represents units' responses determined to be nonsignificant as described above. The spatial arrangement of each grid represents the rough alignment of 32 microelectrodes as they would be implanted in the dorsal aspect of OB per experiment. This ensemble response indicates that most of units show large differences in activation (both positive and negative) with respect to each of the two conditions, (–L) versus clean air, for this particular window in time. This spatial result, when combined with the temporal characteristics seen in Figure 8a–c, is indicative of the higher-order spatio-temporal dynamics that are involved in the encoding of simple odors in OB.

In order to investigate the spatio-temporal differences amongst enantiomers of the same odor we proceeded to create difference plots of the ensemble responses of neurons to each odorant. Figure 8d represents the temporal difference of the ensemble response of 37 single- and multi-units to 200 presentations of 1% (v/v) (+L) subtracted from the ensemble response of the same neurons to 181 presentations of 1% (v/v) (–L) from Animal E. This analysis and statistics is similar to that used to create Figure 8c with two exceptions. The PSTHs start at the alignment of the first inhalation in the presence of each odor at time = 0 and end one second after the alignment. Those units' responses determined *not* to be significantly different between the two cases are marked by a star in Figure 8d using the Wilcoxon nonparametric test at $P < 0.01$ for the specific time period from 0.250 to 0.500 s following the alignment. The false color image of Figure 8d indicates there are a number of neurons that respond to each of the enantiomers of limonene with not only spatial differences but with specific temporal differences as well.

Given the differential activation patterns of these neurons to the enantiomers of limonene as a function of time, we reorganized this information into each neuron's respective position within the electrode array as it was recorded *in vivo* to create Figure 9b. The color of the sections of each circle show the maximal amount of differential activation of the ensemble response to (+L) versus (–L) as seen in the plot of Figure 8d from time 0.335 to 0.340 s following the alignment as determined by two-sample Kolmogorov–Smirnov goodness-of-fit hypothesis test for $P < 0.12$.

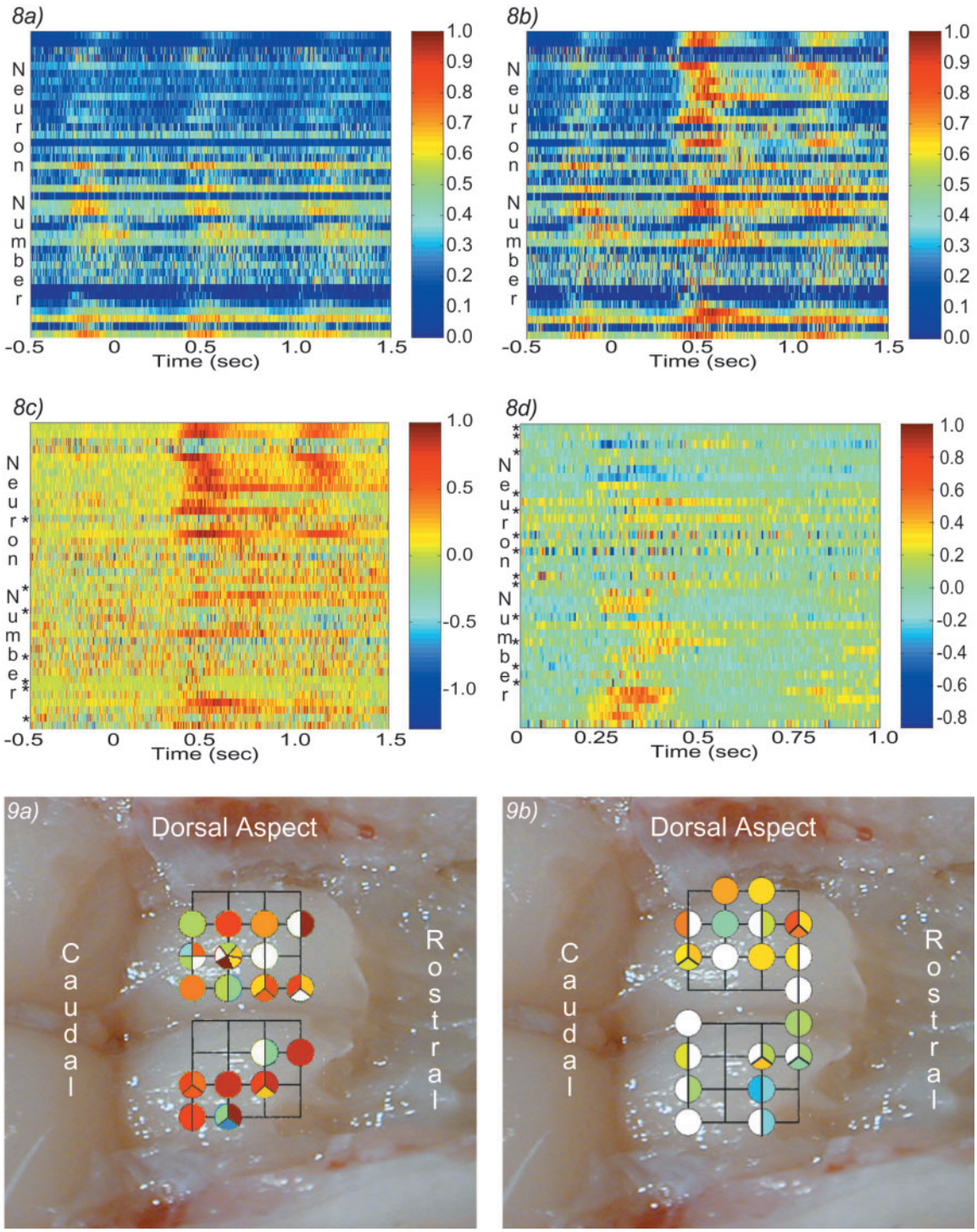

Figure 8 False color PSTHs of 40 neurons aligned to the first inhalation in the presence of **(a)** clean air, **(b)** 1% v/v (–L), data from animal D. Each row is a neuron, each column is a 5 ms bin in the PSTH starting 0.5 s before and ending 1.5 s after alignment. Red and blue colors represent the maximum and minimum firing rates of each neuron, respectively. **(c)** The difference PSTHs between (a) and (b). **(d)** The difference PSTHs between enantiomers of 1% v/v limonene from animal E. Each row is a neuron, each column is a 5 ms bin in the PSTH starting at the alignment and ending 1.0 s after the alignment. Star preceding rows indicate units' response to odor to be nonsignificant.

Figure 9 Spatial activation maps of the simultaneously recorded differences in activation of neurons to **(a)** (–L) and clean air stimulation from animal D and **(b)** (–L) and (+L) stimulation from animal E, in a 5 ms expansion of Figure 8c,d, respectively (see text). Each grid represents an array of 16 electrodes as they were implanted in each hemisphere of OB for a typical experiment. Each circle within the array represents a single electrode with recorded responses. Circles that are partitioned represent an electrode recording more than one unit. The color scales are conserved from Figure 8c,d, respectively. Units with nonsignificant responses to stimulus are colored white.

Discussion

We have developed a device for simultaneously recording from a number of single- and multi-units bilaterally in the dorsal aspect of mammalian olfactory bulb. The technique provides a unique combination of spatial and high temporal resolution data that permits novel statistical analyses of neural responses to odorants which go beyond the scope of this study. One such analysis is the study of synchronous and other temporally correlated events present throughout a spatially distributed ensemble of OB neurons. These spatiotemporal interactions could be significant to an animal's ability to discriminate between odors at low concentration. This technique, as developed to date, has a number of unique advantages in addition to issues that will be discussed below.

Of great concern when applying a microelectrode array to obtain electrophysiological recordings from olfactory bulb is whether the array will cause excessive damage to the bulb during placement. Basic electrophysiological properties of the unit recordings such a peak-to-peak spike amplitude, firing rate, and signal-to-noise ratio are consistent with other cortical recordings obtained from the array and indicate that we are probably recording from viable M/T cells (Chaput and Holley, 1979; Jiang *et al.*, 1996; Maynard *et al.*, 2000). The presence of responding neurons in close proximity to the microelectrodes shortly after insertion and the continued presence of recordings up to 21 h are robust functional indicators that the placement of a large number of electrodes into the bulb can be achieved.

In conducting electrophysiologic investigations, an important aspect of the recordings is their stability. Stable recordings are of particular importance with olfactory investigations because of constraints to the presentation of odors imposed by adaptation phenomena. Additionally, some neurons ceased the firing of action potentials followed by a period of time when they would start firing again. This type of 'waxing and waning' of the response could be explained by the metabolism of the urethane anesthetic agent used (Yu *et al.*, 1993; Jiang *et al.*, 1996). In the former condition this phenomenon did not affect the average relative response to odorant stimulation. In animals A–E, the nasal epithelium was continuously hydrated throughout the recording sessions whereas the epithelia of animals F and G were not, reflecting differences in olfactometers used in these experiments. The addition of hydrated air may have helped to preserve functionality of the epithelium as exhibited by the lower-than-average firing rate recorded from animals F and G. Regardless of the firing rate, responses were consistent for every animal. The presence of consistent populations of neurons and the continuous presence of tracked single units suggest that micro-movements of the array relative to the tissue are not of particular concern with this device. This is probably a consequence of the array distributing shear forces across all electrodes, thus lessening their effect at a given electrode, and the 'floating' design of the array.

The stability of the recordings is not meant to imply that there was no variability in the responses. In all experiments there existed a 'waxing and waning' of unit spontaneous firing rates as a function of time. In addition, each odor presentation was not synchronized to the phase of the animal's breathing and thus the actual start and stop of each odor presentation were randomly distributed in time resulting in variability in the amplitude of the units responses on a trial-by-trial basis. Additionally, when aligning by the inhalation cycle on a trial-by-trial basis, there will be instances where only one inhalation was detected in the presence of odorant and other instances where two inhalations were detected during the odorant presentation time interval. In order to address this issue of variability it would be necessary to initiate an odorant presentation synchronized with the inhalation phase of the animal's breathing. The described array of microelectrodes provides a unique opportunity to investigate trial-by-trial response variability in the neural representations of odors.

An important feature of the technique is that it enables the high-resolution study of the spatio-temporal firing of ensembles of OB neurons. Earlier electrophysiological studies of single OB neurons have shown them to possess highly dynamic responses to odorants (Moulton, 1963; Motokizawa, 1996). Similarly, we have found that during the response of these units to odorant stimulation they can increase or decrease their firing rate over time and that these slow changes are odor specific. A number of units show large differences in rate responses (both positive and negative), even amongst multiple units recorded on the same electrode. Many imaging techniques have indicated broad spatial tuning to odors with glomerulus-specific activation, even amongst enantiomer odor pairs (Xu *et al.*, 2000; Linster *et al.*, 2001; Rubin and Katz, 2001; Spors and Grinvald, 2002). Microelectrode arrays have the ability to record odorant responses of neurons on a spike-by-spike basis from a number of electrodes evenly spaced across the OB. This allows us to investigate the spatial ensemble activation of the output neurons of OB at fine temporal 'slices' simultaneously, following an odorant presentation. The kinetics of the responses of individual neurons in the recorded population can vary greatly, with some neurons 'leading' others 'lagging', and some neurons exhibiting a brief response and others a prolonged response to the 1 s odorant presentation. Not only do these neurons exhibit spatially distinct activation as seen in imaging studies but they also exhibit distinct patterns of temporal activation even amongst enantiomers of the same odor. Only by recording these temporally dynamic responses simultaneously from a number of spatially disparate OB neurons can we begin to understand the significance of these dynamics.

Although we have been able to successfully show acute

recording capabilities of this technology in OB, there exist a number of questions that can only be answered by correlating neural activity with animal behavior. Furthermore, the effects of anesthesia on these recording could be masking the true responses of mitral/tufted cells to odorants possibly by releasing or amplifying inhibition, depending on the type of anesthetic used (Freeman, 1974a). The electrophysiological techniques presented here could be adapted for chronic applications in which these spatio-temporal responses can be recorded over weeks or months in awake-behaving animals. This technology provides a new tool to answer questions pertaining to odor learning and plasticity not possible with current imaging and electrophysiological techniques.

Acknowledgements

In memory of Matthew Sinclair (1982–2002). The authors would like to thank Matthew Sinclair and Michelle Dalton for their assistance with the experiments. Funding for this research was possible through a subcontract from NIDCD SBIR grant #1R43DC04261-01 to Cyberkinetics (Bionic Technologies, LLC) and through a National Research Service Award to the first author through the NIDCD entitled 'Spatio-temporal responses of olfactory bulb neurons'. We also thank Mary T. Lucero, W.C. Michel and Neil J. Vickers for their comments on the manuscript. Drs Edwin Maynard and Richard Normann have a financial conflict of interest with Cyberkinetics, Inc.

References

Belluscio, L. and **Katz, L.C.** (2001) *Symmetry, stereotypy, and topography of odorant representations in mouse olfactory bulbs*. J. Neurosci., 21, 2113–2122.

Bhalla, U.S. and **Bower, J.M.** (1997) *Multiday recordings from olfactory bulb neurons in awake freely moving rats: spatially and temporally organized variability in odorant response properties*. J. Comput. Neurosci., 4, 221–256.

Boulet, M., Daval, G. and **Leveteau, J.** (1978) *Qualitative and quantitative odour discrimation by mitral cells as compared to anterior olfactory nucleus cells*. Brain Res., 142, 123–134.

Campbell, P.K., Jones, K.E., Huber, R.J., Horch, K.W. and **Normann, R.A.** (1991) *A silicon-based, three-dimensional neural interface: manufacturing processes for an intracortical electrode array*. IEEE Trans. Biomed. Engng, 38, 758–768.

Chaput, M.A. (1986) *Respiratory-phase-related coding of olfactory information in the olfactory bulb of awake freely-breathing rabbits*. Physiol. Behav., 36, 319–324.

Chaput, M. and **Holley, A.** (1979) *Spontaneous activity of olfactory bulb neurons in awake rabbits, with some observations on the effects of pentobarbital anaesthesia*. J. Physiol. (Paris), 75, 939–948.

Chaput, M.A. and **Holley, A.** (1985) *Responses of olfactory bulb neurons to repeated odor stimulations in awake freely-breathing rabbits*. Physiol. Behav., 34, 249–258.

Christensen, T.A., Pawlowski, V.M., Lei, H. and **Hildebrand, J.G.** (2000) *Multi-unit recordings reveal context-dependent modulation of synchrony in odor-specific neural ensembles*. Nat. Neurosci., 3, 927–931.

Freeman, W.J. (1974a) *Dynamic patterns of brain cell assemblies. IV. Mixed systems. Oscillating fields and pulse distributions. Pulse-wave problems*. Neurosci. Res. Program Bull., 12, 102–107.

Freeman, W.J. (1974b) *Topographic organization of primary olfactory nerve in cat and rabbit as shown by evoked potentials*. Electroencephalogr. Clin. Neurophysiol., 36, 33–45.

Giraudet, P., Berthommier, F. and **Chaput, M.** (2002) *Mitral cell temporal response patterns evoked by odor mixtures in the rat olfactory bulb*. J. Neurophysiol., 88, 829–838.

Jiang, M., Griff, E.R., Ennis, M., Zimmer, L.A. and **Shipley, M.T.** (1996) *Activation of locus coeruleus enhances the responses of olfactory bulb mitral cells to weak olfactory nerve input*. J. Neurosci., 16, 6319–6329.

Johnson, B.A., Woo, C.C. and **Leon, M.** (1998) *Spatial coding of odorant features in the glomerular layer of the rat olfactory bulb*. J. Comp. Neurol., 393, 457–471.

Jones, K.E., Campbell, P.K. and **Normann, R.A.** (1992) *A glass/silicon composite intracortical electrode array*. Ann. Biomed. Engng, 20, 423–437.

Katoh, K., Koshimoto, H., Tani, A. and **Mori, K.** (1993) *Coding of odor molecules by mitral/tufted cells in rabbit olfactory bulb. II. Aromatic compounds*. J. Neurophysiol., 70, 2161–2175.

Kay, L.M. and **Laurent, G.** (1999) *Odor- and context-dependent modulation of mitral cell activity in behaving rats*. Nat. Neurosci., 2, 1003–1009.

Lei, H., Christensen, T.A. and **Hildebrand, J.G.** (2002) *Local inhibition modulates odor-evoked synchronization of glomerulus-specific output neurons*. Nat. Neurosci., 5, 557–565.

Leveteau, J. and **MacLeod, P.** (1966) *Olfactory discrimination in the rabbit olfactory glomerulus*. Science, 153, 175–176.

Linster, C., Johnson, B.A., Yue, E., Morse, A., Xu, Z., Hingco, E.E., Choi, Y., Choi, M., Messiha, A. and **Leon, M.** (2001) *Perceptual correlates of neural representations evoked by odorant enantiomers*. J. Neurosci., 21, 9837–9843.

Maynard, E.M., Fernandez, E. and **Normann, R.A.** (2000) *A technique to prevent dural adhesions to chronically implanted microelectrode arrays*. J Neurosci. Methods, 97: 93–101.

Motokizawa, F. (1996) *Odor representation and discrimination in mitral/tufted cells of the rat olfactory bulb*. Exp. Brain Res., 112, 24–34.

Moulton, D.G. (1963) *Electrical activity in the olfactory system of rabbits with indwelling electrodes*. In Zotterman, Y. (ed.), Olfaction and Taste. Pergamon Press, Oxford, pp. 71–84.

Moulton, D.G. and **Tucker, D.** (1964) *Electrophysiology of the olfactory system*. Ann. N. Y. Acad. Sci., 116, 380–428.

Onoda, N. and **Mori, K.** (1980) *Depth distribution of temporal firing patterns in olfactory bulb related to air-intake cycles*. J. Neurophysiol., 44, 29–39.

Paxinos, G. (1998) The Rat Brain in Stereotaxic Coordinates. Academic Press, San Diego, CA.

Rousche, P.J. and **Normann, R.A.** (1992) *A method for pneumatically inserting an array of penetrating electrodes into cortical tissue*. Ann. Biomed. Engnf, 20, 413–422.

Rubin, B.D. and **Katz, L.C.** (2001) *Spatial coding of enantiomers in the rat olfactory bulb*. Nat. Neurosci., 4, 355–356.

Slotnick, B.M. and **Nigrosh, B.J.** (1974) *Olfactory stimulus control evaluated in a small animal olfactometer*. Percept. Motor Skills, 39, 583–597.

Slotnick, B.M. and **Ptak, J.E.** (1977) *Olfactory intensity-difference thresholds in rats and humans*. Physiol. Behav., 19, 795–802.

Spors, H. and **Grinvald, A.** (2002) *Spatio-temporal dynamics of odor representations in the mammalian olfactory bulb*. Neuron, 34, 301–315.

Stewart, W.B., Kauer, J.S. and **Shepherd, G.M.** (1979) *Functional organization of rat olfactory bulb analysed by the 2-deoxyglucose method*. J. Comp. Neurol., 185, 715–734.

Xu, F., Kida, I., Hyder, F. and **Shulman, R.G.** (2000) *Assessment and discrimination of odor stimuli in rat olfactory bulb by dynamic functional MRI*. Proc. Natl Acad. Sci. USA, 97, 10601–10606.

Yu, G.Z., Kaba, H., Saito, H. and **Seto, K.** (1993) *Heterogeneous characteristics of mitral cells in the rat olfactory bulb*. Brain Res. Bull., 31, 701–706.

Accepted May 29, 2003